Faculty of Science and Engineering

Neha Rajendra Bari Tamboli

Research Internship in Computing Science

Supervisors

Prof. Dr. Michael Biehl

M.Sc Michiel Straat

Order parameter based study of Hidden unit specialization in Neural Networks for ReLU and Sigmoidal activation functions

October 2020

Bernoulli Institute for Mathematics, Computer Science and Artificial Intelligence

Chapter 1

Introduction

The recent popularity in deep learning has opened an advanced gateway to solving the state-of-the-art subset of dynamic tasks like object detection and speech recognition. This subset of tasks occur across various domains like stock market, medical science and military applications. Deep learning allows computational models that are composed of multiple hidden layers to learn representations of data with multiple levels of abstraction (LeCun et al. 2015). Shallow neural networks consist of one hidden layer instead of multiple hidden layers. These form a toy-model which can be exactly solved to study deep neural networks which have largely been used as black boxes (Angelov and Sperduti 2016, Goodfellow et al. 2016, Prajit Ramachandran 2017).

In this work we study the generalization properties of a shallow neural network as a function of the size of the dataset. We consider a student-teacher model training scenario in which we train the student network and observe the overlap between its weights and the weights of the teacher neural network. In order to understand the learning behaviour of the student neural network, we invoke the celebrated statistical mechanics (Gibbs 1902) theory of physics which gives us the tools to understand the macroscopic behaviors of a system using certain averages over the properties of the microscopic constituents of the system. Specifically, we use statistical mechanics inspired method of tracking the order parameters to spot a phase transition in the network. These order parameters enable us to track the learning behaviour without having to track the individual weights, i.e. they give us a macroscopic view of learning. The activation functions used for this experiment are the ReLU and the shifted sigmoid. We analyse systems of two different sizes and observe differences in student's learning behaviour for these activation functions. We also make comparison with theoretical results based on statistical mechanics of

equilibrium and the central limit theorem.

Chapter 2

Methods

2.1 Experiment Setup

We consider a shallow artificial feed-forward neural network with one hidden layer comprising of K hidden units, N input units and one linear output unit. The input nodes are connected to each hidden unit via edges that have adaptive weights. Therefore there are $N \times K$ weights between input and hidden units and K weights between hidden to output unit. Weights can be aggregated as weight vectors by introducing the notation $\boldsymbol{w_k} \in R^N$, whose components include all weights going to the k^{th} hidden unit, where $k = 1..K$. The hidden unit performs a weighted sum of the components and normalization of input vector followed by the application of an activation function. Weights connecting hidden to output units are all unity. Therefore, the output simply adds the incoming activations and normalizes the sum.

The main aim is to study how closely the weights of a neural network called "student" resemble another neural network called "teacher", upon training. The teacher neural network has randomly generated weights, identical architecture and is not trained. Moreover, the student neural network is trained on the labels generated by the teacher. The aim of the learning is not only to learn the examples, but to learn the underlying function that produces the targets for the learning process (Krogh and Hertz 1992).

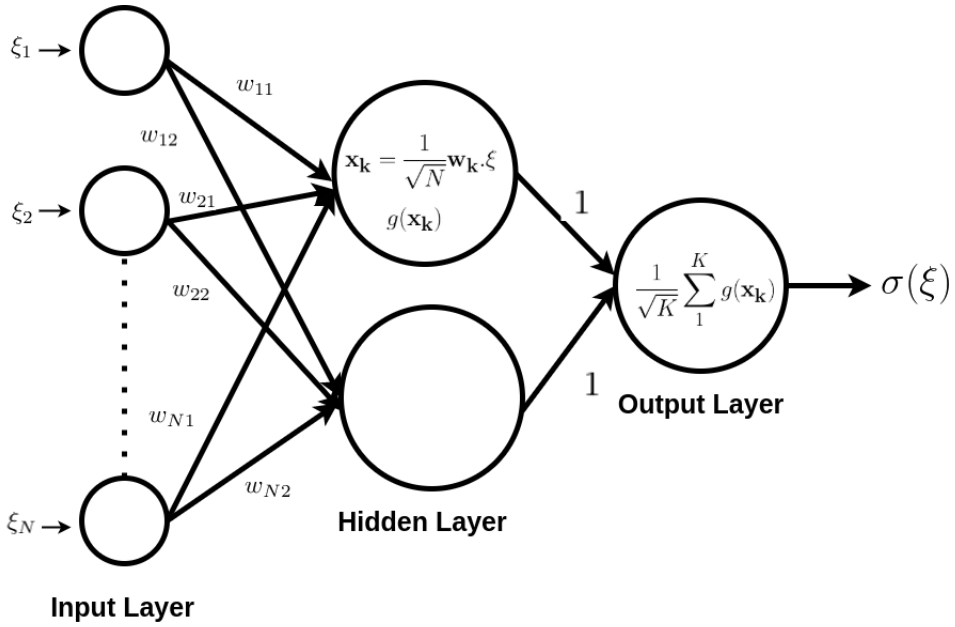

Figure 2.1: Schematic representation of the architecture of student and teacher neural networks with N input units, one hidden layer with $K = 2$ units and one linear output unit. The individual neurons in the hidden unit execute a weighted sum of inputs to compute the local potential x_k and apply an activation function g on it. The sum is normalized by $\sqrt{N}$ to keep the norm of the local potential of $\mathcal{O}(1)$. The output neuron acts as an aggregator and computes the sum of activations. This sum is normalized by $\sqrt{K}$ such that it approaches $\mathcal{O}(1)$. The output is given by $\sigma(\xi)$ and is continuous. This neural network thus performs regression.

2.2 Activation function

The main goal of this report is to study generalization properties of the student neural network under two different types of activation functions. The first one called Rectified Linear Unit (ReLU) is defined as $max(0, x)$:

$$g(x) = \begin{cases} 0, & \text{if } x < 0, \\ x & \text{elsewhere.} \end{cases} \tag{2.1}$$

Therefore the function maps $\mathbb{R} \to \mathbb{R}^+$, making it unbounded. The derivative of ReLU is defined as follows:

$$g'(x) = \begin{cases} 0, & \text{if } x < 0, \\ 1 & \text{if } x > 0. \end{cases} \tag{2.2}$$

The ReLU activation function is not differentiable at $x = 0$, however this does not affect us computationally because of floating point precision. In our simulations we define the derivative to be 1 at $x = 0$. This function is also called the ramp function and is analogous to half

wave rectification in electrical engineering. This activation function has strong motivation from biology (Hahnloser et al. 2000).

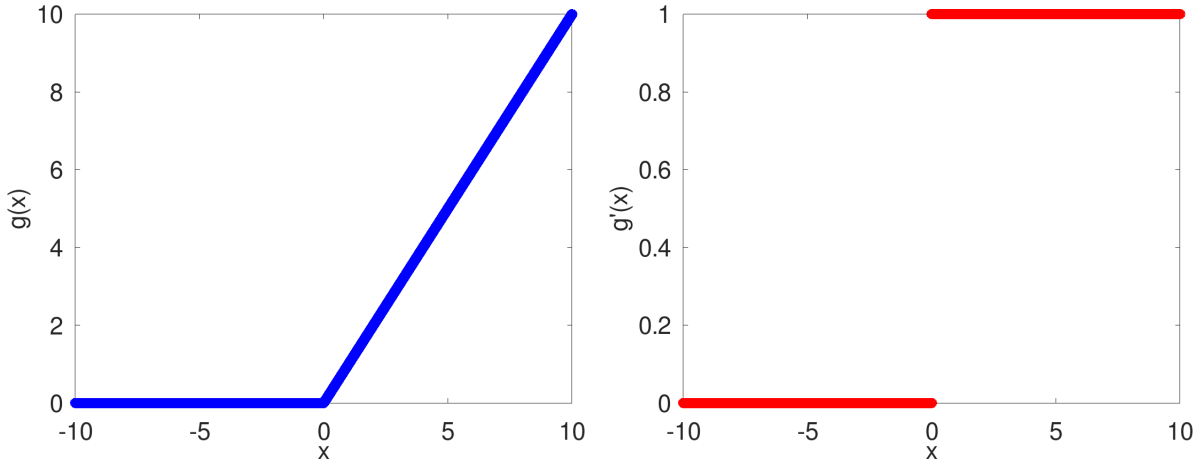

(a) The ReLU activation function.

(b) Derivative of the ReLU activation function.

Figure 2.2: The ReLU activation function and its derivative. The x-axis represents the local potential.

The advantages of ReLU activation function includes:

- biological plausibility.
- efficient computation & sparse representation.
- fewer vanishing gradient problems compared to sigmoid which saturates asymptotically in both directions (fig2.3).
- scale invariance: $max(0, \gamma x) = \gamma max(0, x)$ for $\gamma > 0$.

The second activation function is the sigmoid activation function. For the purpose of this work we use the shifted erf (Ahr et al. 1998) function defined as:

$$g(x) = 1 + erf\left(\frac{x}{\sqrt{2}}\right). \tag{2.3}$$

Its derivative is given by:

$$g'(x) = \sqrt{\frac{2}{\pi}} e^{\frac{-x^2}{2}}. \tag{2.4}$$

The shifted sigmoid activation function maps $\mathbb{R} \to [0, 2]$, making it bounded. Additionally, the function is differentiable everywhere and monotonically increasing.

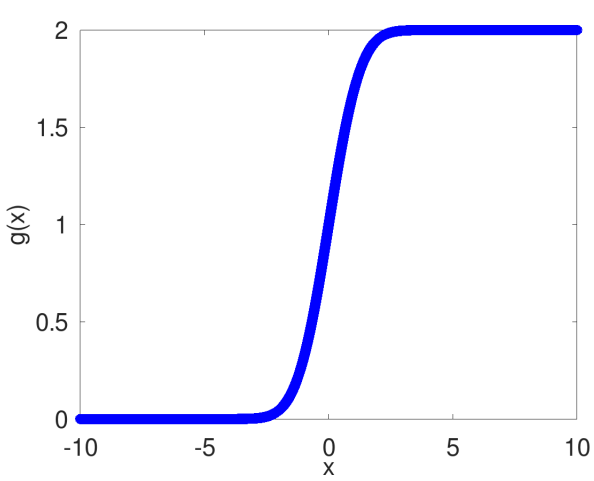

(a) The erf activation function.

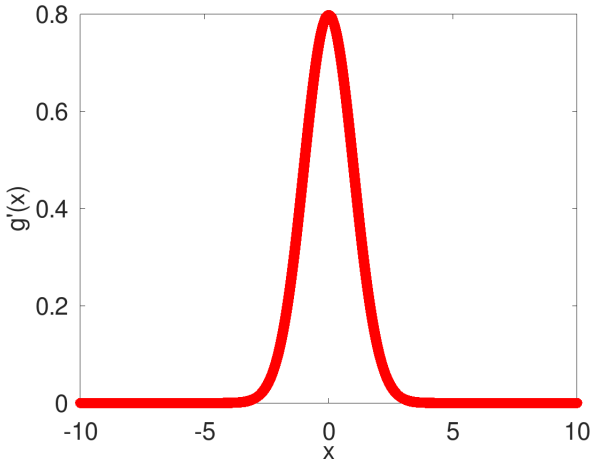

(b) The gaussian derivative of erf activation function.

Figure 2.3: The shifted sigmoid activation function realised as a shifted erf function and its derivative.

2.3 Student-teacher scenario

This experiment involves two networks namely, the Student and the Teacher network. They have similar architecture shown in fig 2.1. We randomly generate the weights of the teacher neural network. These weights are drawn from a normal distribution and are denoted by $\mathbf{w_k^*} \in \mathbb{R}^N$. The teacher network acts on the input data to generate a label, which is what the student network is eventually trained on. The randomly generated teacher weight vectors are orthonormalized using the Gram-Schmidt procedure (Golub and Van Loan 1996).

$$\boldsymbol{w_m^*} \cdot \boldsymbol{w_n^*} = \delta_{mn}, \text{ where } \delta_{mn} = \begin{cases} 1, & \text{if } m = n, \\ 0, & \text{if } m \neq n \end{cases} \tag{2.5}$$

is the kronecker delta function. Input vector corresponding to the μth example is given by $\boldsymbol{\xi^\mu}$. Each input vector is N dimensional to make it commensurate with the dimension of the input layer of the neural network. Furthermore, we choose $\boldsymbol{\xi^\mu}$ such that each component is drawn from a normal distribution, just like the weights.

The training set matrix used to train the student network is $D = \{\boldsymbol{\xi^\mu}, \tau^\mu\}_1^P$, where τ represents the teacher network generated label. Here, P is the number of examples.

The quantity

$$\alpha = \frac{P}{KN} \tag{2.6}$$

scales the number of examples in the dataset as $P = \alpha\ K\ N$. The detailed effects of increase in the number of examples on learning is elaborated in the results section.

The local potential for the teacher network is represented by

$$x_m^* = \frac{1}{\sqrt{N}} \boldsymbol{w_m^*} \cdot \boldsymbol{\xi} \tag{2.7}$$

where $\boldsymbol{w_m^*}$ is the weight vector corresponding to the m^{th} hidden unit and $m = 1..M$, where M are the number of hidden units in the teacher network . The local potential is fed to the choice of activation function and then aggregated by the output unit to generate the output label

$$\tau(\boldsymbol{\xi}) = \frac{1}{\sqrt{M}} \sum_{m}^{M} g(x_m^*) \tag{2.8}$$

where, τ is the final teacher output. For the sake of simplicity, the current simulation deals with $K = M$. Other configurations where $K \neq M$ can also be studied but are not covered here.

2.4 Loss function

The cost that penalizes the errors is represented in terms of the quadratic loss function (Berger 1985). The cost determines how good the student is at predicting teacher labels. The cost function is represented as,

$$\epsilon(\boldsymbol{\xi}) = \frac{1}{2}(\sigma(\boldsymbol{\xi}) - \tau(\boldsymbol{\xi}))^2 \tag{2.9}$$

Cost function is applied on each example where $\sigma(\boldsymbol{\xi})$ is the student output and $\tau(\boldsymbol{\xi})$ is the teacher output per example. The cost calculated is then summed over for all the examples to calculate the training error for the entire training set. It is defined as below,

$$E = \sum_{\mu=1}^{P} \epsilon(\boldsymbol{\xi}^{\mu}). \tag{2.10}$$

where $\boldsymbol{\xi}$ refers to the current example input vector taken into consideration for computing the cost.

2.5 Stochastic Gradient Descent

The student neural network is trained using the stochastic gradient descent (SGD) algorithm (Robbins and Monro 1951), to estimate the parameters of the student adaptive weights iteratively, that minimize the cost function. During each iteration in the training process, the network starts from a randomly selected example $\boldsymbol{\xi}$ from a set of P examples, it then computes the student label $\sigma(\boldsymbol{\xi})$ using forward propagation to calculate the cost function. The teacher label is pre-calculated for every example. It then moves the weights by a step proportional to the negative of the gradient of the cost function with respect to the weights (i.e. in the direction of steepest descent of the cost function). At the training step $i+1$ when a particular example ξ is chosen, the weight matrix is given by,

$$\boldsymbol{w}_k^{i+1} = \boldsymbol{w}_k^i - \frac{\eta \boldsymbol{\nabla}_{\boldsymbol{w}_k^i} \epsilon(\boldsymbol{\xi})}{N}. \tag{2.11}$$

for $k = 1...K$. Here, η is called the learning rate. After, every step the student weight vector associated with the hidden unit j is normalized as below:

$$\left|\boldsymbol{w_k}\right| = \sqrt{N} \tag{2.12}$$

SGD performs frequent updates with a high variance that cause the objective function to fluctuate heavily (Ruder 2016). Therefore tuning a reasonable learning rate η is important. If η is too large, the network will fluctuate far from the global minima and never converge. If η is too small the network will never learn. In our experiments we heuristically tuned η to be equal to 0.5 and 0.8 for different systems. The learning process is terminated when the decrease in the loss function for a set prolonged period of time is negligible or when a required number of training steps have been taken. To evaluate the derivative of the loss function (2.10) w.r.t to the weights we invoke the celebrated backpropagation method (Rumelhart et al. 1986, Kelly 1960):

$$\nabla_{\boldsymbol{w}_k^i}\ \epsilon = (\sigma - \tau) g'(\boldsymbol{w}_k^i \cdot \boldsymbol{\xi}) \boldsymbol{\xi} \tag{2.13}$$

The training process is described in the pseudocode below;

Listing 2.1: Psuedocode for NN training using Stochastic gradient descent

```
for i to training steps:
  %one random example at a time
  example = randi(dataset);
        %forward prop

        local_potential = dot(example,weights)/(\sqrt(N))
        psi(example)= sum(activation_function(local_potential))/(\sqrt(K))

        %backprop
        gradient = (psi(example) - tau(example))*  derivative(local_potential)*
    example;

        %update
        new_weights(example) =  (weights(example)) - ((learning_rate/N)*
    gradient);

        %weight normalization
        new_weights(example) = new_weights(example)./norm(new_weights(example))
    ;
end
```

2.6 Generalization error

The generalization error measures the degree to which a neural network is able to adapt itself on a novel dataset. The network should not only learn the training data, but it should be able to predict labels on novel data (test data). If a network performs well on the training data but does not generalize well on the unseen data, the model is said to overfit. When the network does not train well on the training dataset and neither does it generalize well on the unseen data, it is commonly referred to as under-fitting. The goal is to reduce the generalization error without under-fitting or over-fitting the model.

The mathematical model for generalization error is represented as

$$\epsilon_g = \frac{1}{2K}\left\langle \left(\sum_{i=1}^{K} g(x_i) - \sum_{j=1}^{K} g(x_j^*) \right)^2 \right\rangle \tag{2.14}$$

The generalization error is the expectation value of the quadratic deviation between the student and the teacher output. It computes the average over the joint density over x_i & x_j^* which fundamentally is a gaussian average. The gaussian average can be computed in terms of the order parameters for both ReLU (A.1) (Michiel Straat 2018, Oostwal et al. 2021) and sigmoid

(A.2) (Saad and Solla 1995).

2.7 Order parameters

An order parameter distinguishes two different phases (or orders). Typically an order parameter has different values for different phases. For our experiments, we need to keep track of how student weights change as learning progresses. Here, order parameters come in handy as a few of them are sufficient to describe learning in large systems. We now derive order parameters (Biehl et al. 1998, Ahr et al. 1998) from weight vectors to track the progress in learning.

The order parameter Q_{ij} is the student overlap, defined as:

$$Q_{ij} = \frac{\boldsymbol{w_i} \cdot \boldsymbol{w_j}}{N} \tag{2.15}$$

and

$$Q_{ij} = \begin{cases} 1, & \text{if } i = j, \\ C, & \text{if } i \neq j. \end{cases} \tag{2.16}$$

The overlap between identical student vectors is 1, while non-identical students overlap at a scalar value C.

Similarly, the order parameter R_{ij} is the student-teacher overlap.

$$R_{ij} = \frac{\boldsymbol{w_i} \cdot \boldsymbol{w_j^*}}{N} \tag{2.17}$$

and,

$$R_{ij} = \begin{cases} R, & \text{if } i = j, \\ S, & \text{if } i \neq j. \end{cases} \tag{2.18}$$

The assumptions in equations (2.16) and (2.18) simplify the consideration of specialization as well as anti-specialization of the hidden units. The special consideration of $i = j$ singles out one optional specialization but all the others are equivalent.

The phases can be represented as below;

The $\boldsymbol{R = S}$ phase represents a barren plateau, in this phase the neural network does not specialize in learning. All the student vectors have equal overlap with all the teacher vectors, due to which they never really learn in respect to a single teacher.

The $\boldsymbol{R > S}$ represents specialization, i.e. as per equation (2.18), the $i = j$ student-teacher pair have maximum overlap with each other and the student learns with respect to their equal indexed teacher vector.

The $\boldsymbol{R < S}$ represents anti-specialization. As per equation (2.18), the student vector shows minimum overlap (negative) with the teacher vectors when the index $i = j$, where as the student vector is weakly positively overlapped with the teacher vectors such that index $i \neq j$.

The normalization and orthogonal property of the student and teacher weight vectors as per (2.12) and (2.5) obey the property that the generalization error can be represented in terms of order parameters as (A.1) and (A.2). The order parameters lie between -1 and 1.

$$-1 \leq Q_{ij}, R_{ij} \leq 1 \tag{2.19}$$

2.8 Training of Student Neural Network

The plots in fig 2.4 depict the training of a student neural network in the student teacher scenario using stochastic gradient descent. We use the ReLU activation function in the hidden units. The first plot depicts the generalization error ϵ_g as a function of training steps. We can clearly spot a plateau region where the graph ϵ_g is almost flat. Additionally, both diagonal and off-diagonal elements of R_{ij} have essentially the same values signalling poor generalization. As training steps progress, the system eventually specializes well, as evident from the diagonal values of R_{ij} i.e. R_{11} and R_{22} reaching their maximum value of 1 and off-diagonal elements R_{12} and R_{21} reaching 0. This results in a further decrease of ϵ_g and eventual convergence to $\approx 10^{-6}$. The training error E follows a trend similar to ϵ_g. In the fig 2.5, we report similar plots for $\alpha = 1$. Here, we see that both ϵ_g and E stagnate into a plateau state, i.e. the student network never generalizes well. This is evident from looking at the student-teacher overlap R_{ij} vs training steps. The diagonal elements of R_{ij} saturate at 0.5, instead of going to 1 and the off diagonal elements saturate at around 0.2, instead of going to zero. To obtain these plots the values N, η and the number of training steps were chosen heuristically after several trials.

The generalization achieved in this training is very sensitive to α which controls the dataset size P. Studying the behaviour of student neural network as a function of α is the central goal of this report. Armed with statistical mechanics inspired tools, i.e. the student-teacher order parameter R_{ij}, we report the learning curves in the next section.

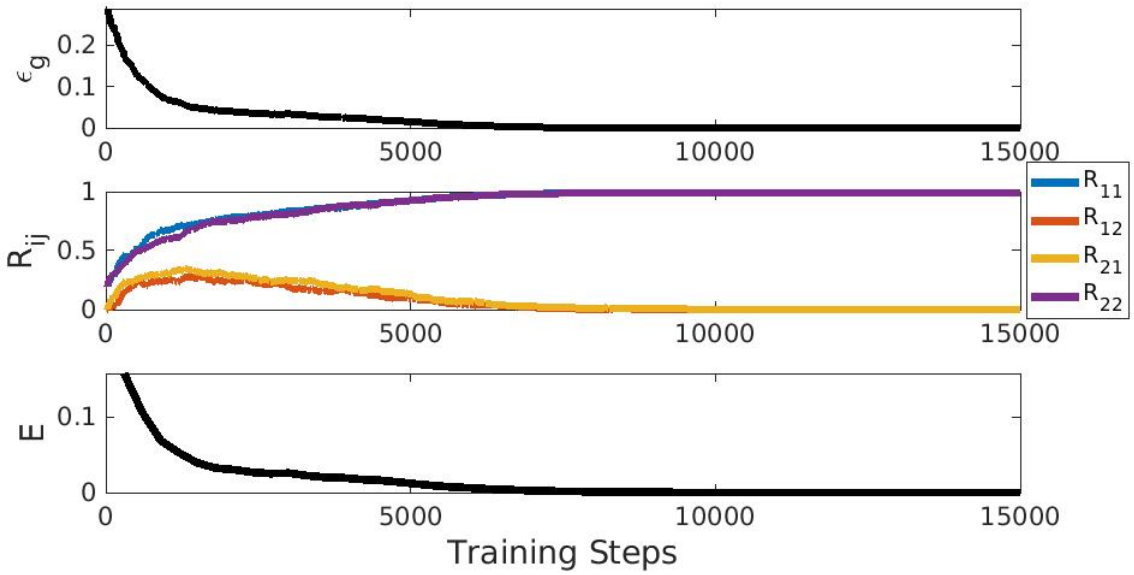

Figure 2.4: Training of student neural network with $N = 100$ input units, $K = 2$ hidden units at a dataset size scaling parameter $\alpha = 8$ and learning rate $\eta = 0.5$ using stochastic gradient descent. Top plot depicts the generalization error ϵ_g as a function of training steps. Middle plot depicts student-teacher overlap parameters R_{ij}. Bottom plot depicts training error E as a function of training steps. At the end of the training the $\epsilon_g = 5.135\times10^{-6}$ and $E = 2.8964\times10^{-6}$.

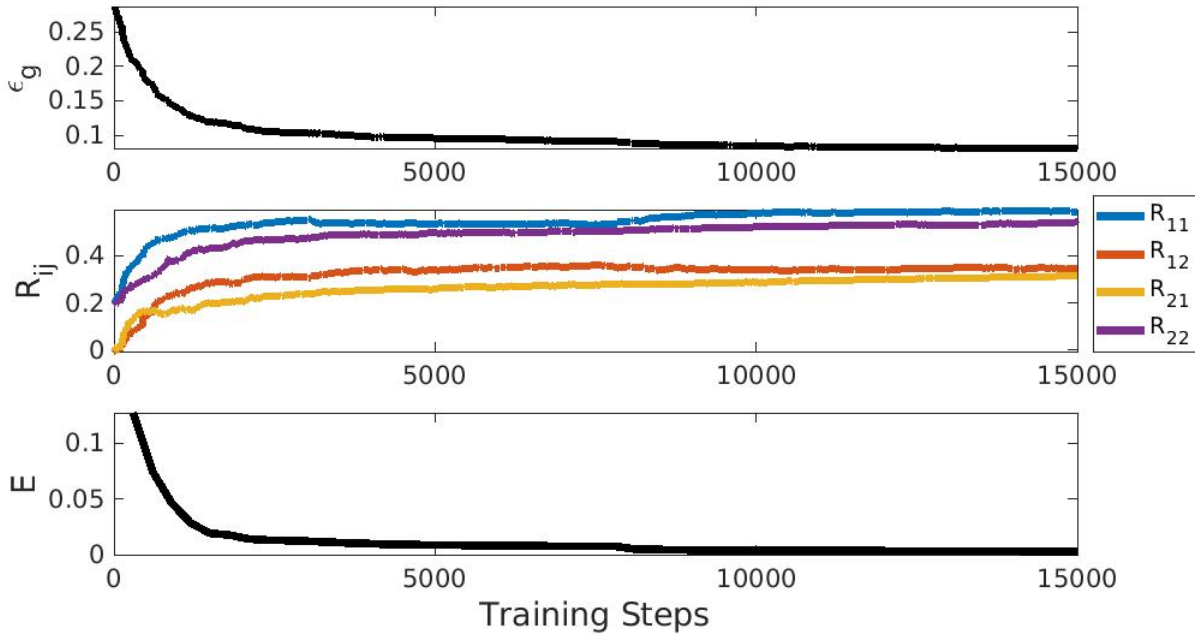

Figure 2.5: Training of student neural network with $N = 100$ input units, $K = 2$ hidden units at a dataset size scaling parameter $\alpha = 1$ and learning rate $\eta = 0.5$ using stochastic gradient descent. Top plot depicts the generalization error ϵ_g as a function of training steps. Middle plot depicts student-teacher overlap parameters R_{ij}. Bottom plot depicts training error E as a function of training steps. At the end of the training the $\epsilon_g = 0.1069$ and $E = 0.0052$. The ϵ_g decreases rapidly initially, but eventually stagnates and the plateau state appears to be the only solution.

Chapter 3

Results

In this section we will report the generalization error achieved by the student network as a function of α for two different hidden layer sizes $K = 2$ and $K = 5$. Additionally, to understand the behaviour of student units w.r.t. the teacher units we will report the student-teacher overlap order parameters as a function of α. The $K = 2$ system serves as the first example where a phase transition between states with poor generalization and states with good generalization is spotted qualitatively. In the research leading to this report we studied systems with $K = 2$ to 5. However, it's the $K = 5$ system where we first see anti-specialization behaviour for ReLU activation function. Phase transitions are spotted in this system simulation as well, at least qualitatively.

We begin by reporting the initial conditions which lead to specialization and anti-specialization behaviour for different systems.

3.1 Initial conditions

Initial conditions play a crucial role in determining if the system will specialize or anti-specialize.

3.1.1 Specialization

For achieving a specialized state where R and Q follow the conditions as per (2.18 and 2.16) the initial condition for $K = 2$ **and** $K = 5$ systems for both ReLU and sigmoid are,

$$Q = (I_{K\times K}) \text{ and } R = 0.2(I_{K\times K}). \tag{3.1}$$

where $Q_{ii} = 1$ and $Q_{ij} = 0$ for $i \neq j$ while $R_{ii} = 0.2$ and $R_{ij} = 0$ for $i \neq j$.

3.1.2 Anti-specialization

In Anti-specialization the student vectors are anti aligned with corresponding teacher vector (i.e. their dot product is negative). The student learns the adaptive weights of corresponding teacher with which it has highest negative dot product. The initial conditions used for anti-specialization are as below for $K = 5$ system.

$$Q = I_{K\times K} + (0.04)(J_{K\times K} - I_{K\times K}); \tag{3.2}$$

$$R = -0.001I_{K\times K} + (0.1)(J_{K\times K} - I_{K\times K}); \tag{3.3}$$

Where J is a matrix of all ones. Here, the student vector has a unity overlap with itself ($Q_{ii} = 1$) and it has a non-zero overlap with the other student vectors ($Q_{ij} = 0.4$ for $i \neq j$).

R parameter configuration satisfies the condition $R < S$ for anti-specialization. Equation (3.3) shows that the corresponding ($i = j$) student-teacher vectors are negatively aligned while the remaining vectors are weakly positively aligned. The student vector has an overlap of -0.0010 with its corresponding teacher vector (R_{ii}) and it has a non-zero overlap of 0.1000 with the remaining teacher vectors (R_{ij} for $i \neq j$).

The conditions laid out were found through trial and error using intuition from the definition of order parameters.

3.2 Simulation of learning in matched student-teacher scenario

We now report the main results on learning in the student neural networks in the matched student-teacher scenario. In these simulations we use $N = 100$ and 600, $K = 2$ and 5 and a learning rate of 0.5 and 0.8. For reference, a system with $K = 5$, $N = 600$ and $\alpha = 20$, implies a dataset size of $P = \alpha KN = 60,000$ examples . For the system size $K = 2$ we repeat the simulation for 30 iterations for 25,000 training steps for each alpha and report the averages along with standard deviation (error bars). For larger system size i.e. $K = 5$ we repeated the

simulations for 10 iterations for $90,000$ training steps for each alpha. The number of iterations here is less because of the time required to conduct these simulations.

3.2.1 Generalization Error for K=2 system

For the case $K = 2$ we obtain the learning curves for perfectly matching student-teacher scenario, shown in fig 3.1. To produce these plots we followed the recipe laid out in the previous section, for every α. Plot (a(b)) of fig 3.1 shows ϵ_g as a function of α for the ReLU(sigmoid) activation function. Here, we take the ϵ_g value at the mid-point (midpoint of the region where the loss values are almost constant) of the plateau as shown in fig 2.4. For the converged ϵ_g we simply take the end-point.

3.2.2 Converged and plateau states for K=2 system

Using the initial conditions for the $K = 2$ system (3.1.1), during the learning process the neural network gets stuck in the plateau states initially. This is an unspecialized state and can be observed in the figure (3.2a) for ReLU from $\alpha \approx 1$ to $\alpha \approx 3$ and in figure (3.2c) for sigmoid from $\alpha \approx 5$ to $\alpha \approx 6$ approximately where R and S barely vary. Both the student hidden units learn little information about the corresponding teachers.

Once the plateau states are overcome, the student network starts learning more efficiently. Theory from (Oostwal et al. 2021) predicts that a phase transition occurs in this regime. Each student vector largely overlaps with exactly one teacher vector. This represents the specialized phase where $R_{ij} = 1$ for $i = j$ and zero for $i \neq j$. This can be observed for ReLU in (3.2a) for $\alpha \approx 4$ and for sigmoid in (3.2c) for $\alpha \approx 6$.

The generalization error (3.1) starts to rapidly decrease when the student units start to specialize. Predictions from theory (Oostwal et al. 2021) are more precise as there the authors use the limit $N \to \infty$, there a sharp kink appears due to the large system size. After the kink, the ϵ_g decreases rapidly. In the plot above, the ϵ_g converges to $7.845e-11$ for $\alpha = 16$ for ReLU and to $1.4611e-04$ for sigmoid at $\alpha = 23$.

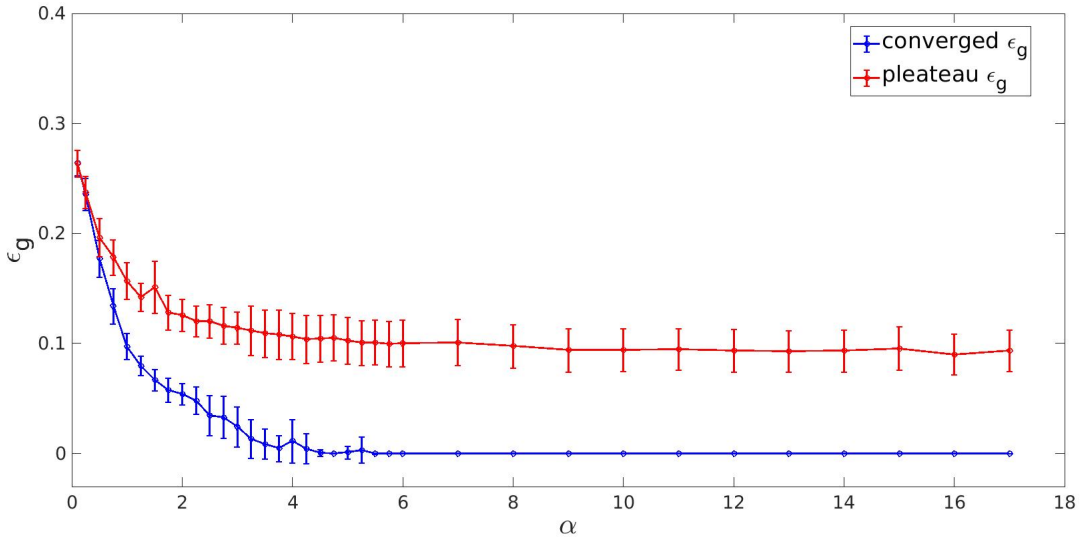

(a) ϵ_g for ReLU

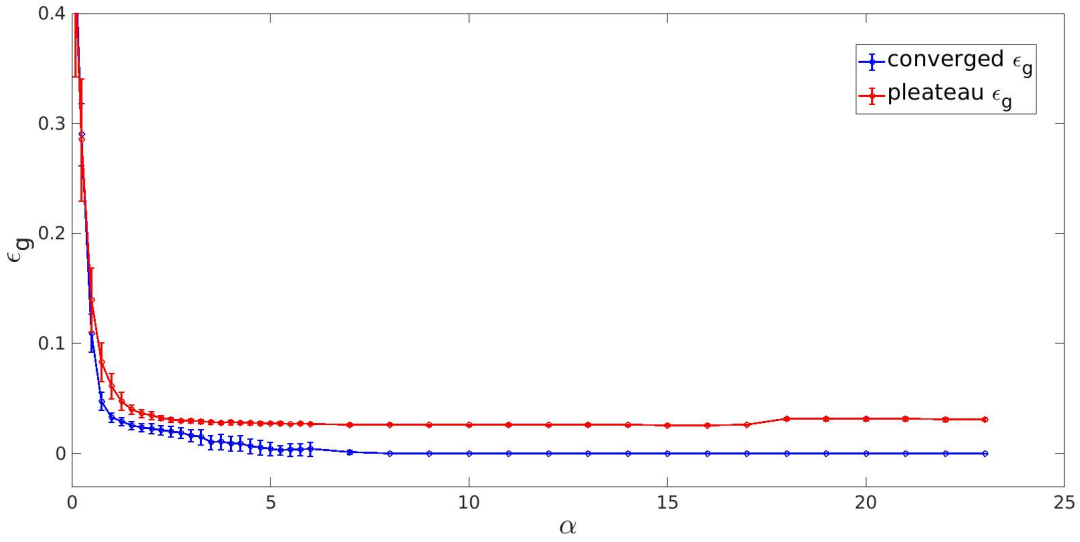

(b) ϵ_g for Sigmoid

Figure 3.1: The generalization errors of converged and plateau states ϵ_g for ReLU and sigmoid activation function with $K = 2$ hidden units as a function of α. The plateau(converged) states are unspecialized and lead to worse(better) generalization.

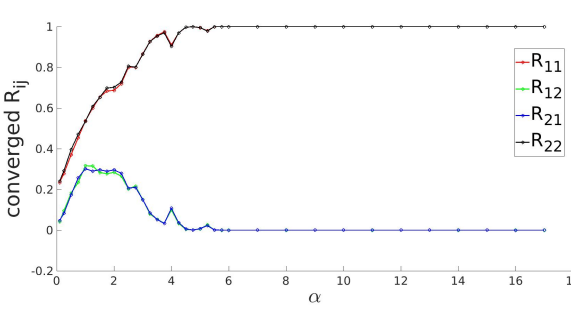

(a) ReLU converged

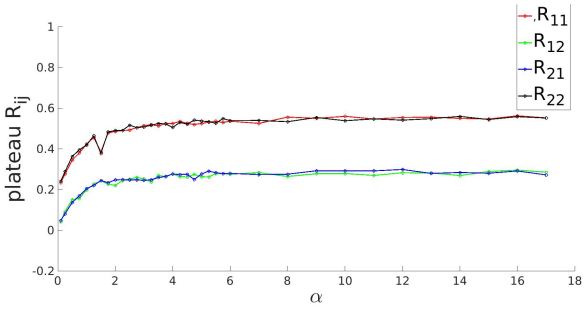

(b) ReLU plateau

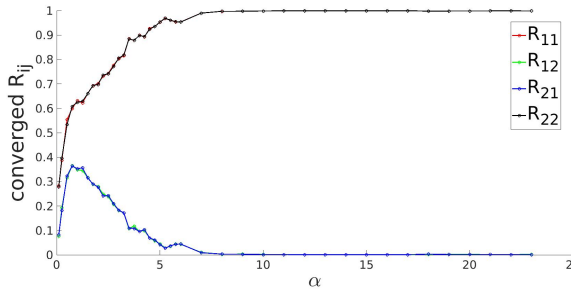

(c) Sigmoid converged

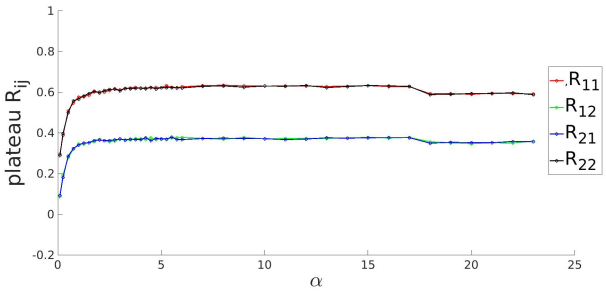

(d) Sigmoid plateau

Figure 3.2: The student-teacher overlap order parameters R_{ij} for student teacher system where both system have 2 hidden units as a function of α (which governs the dataset size). The converged parameters(a,c) show that after an initial period of bad generalization, the diagonal order parameters approach 1 and the off-diagonal parameters approach 0, signalling specialization. For the plateau states, order parameters saturate at 0.5, signalling that no specialized solution is achieved.

3.3 K=5 system

We now move to a larger system size. Here we report the plots of student-teacher overlap matrix R_{ij} with ReLU activation first and then the generalization error. Then we report results for the sigmoid activation function in a similar fashion. For a $K = 5$ system the R matrix has 25 entries. To make comparisons easier we plot all doagonal elements with black color.

3.3.1 Converged state for K=5 system with ReLU activation function

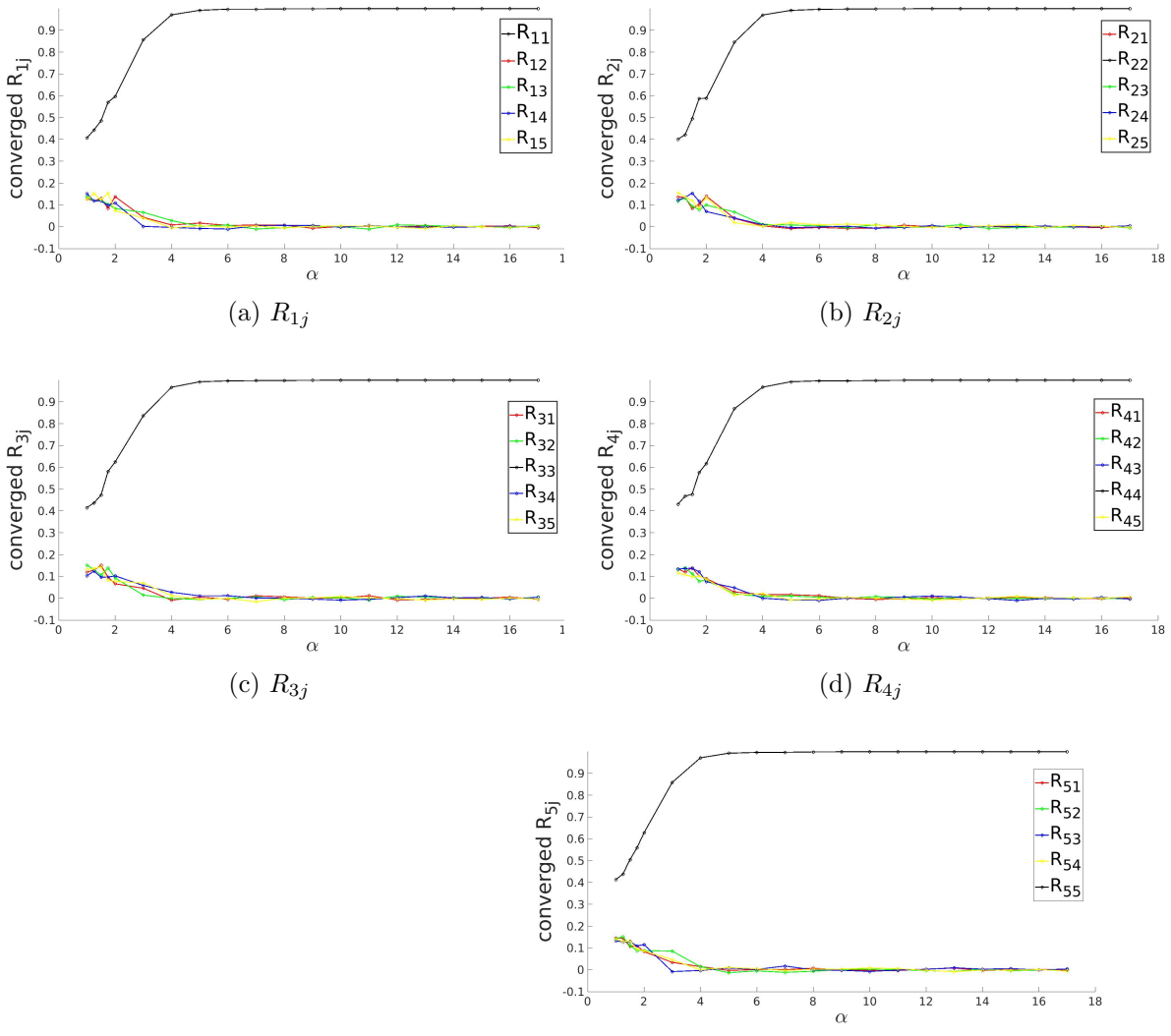

(a) R_{1j} (b) R_{2j}

(c) R_{3j} (d) R_{4j}

(e) R_{5j}

Figure 3.3: Row-wise plot of student-teacher overlap order parameter matrix at the converged ϵ_g. The diagonal elements of R_{ij} (in black) approach the value of 1 and off-diagonal elements approach 0 as α increases, signalling specialization.

3.3.2 Plateau state for K=5 system with ReLU activation function

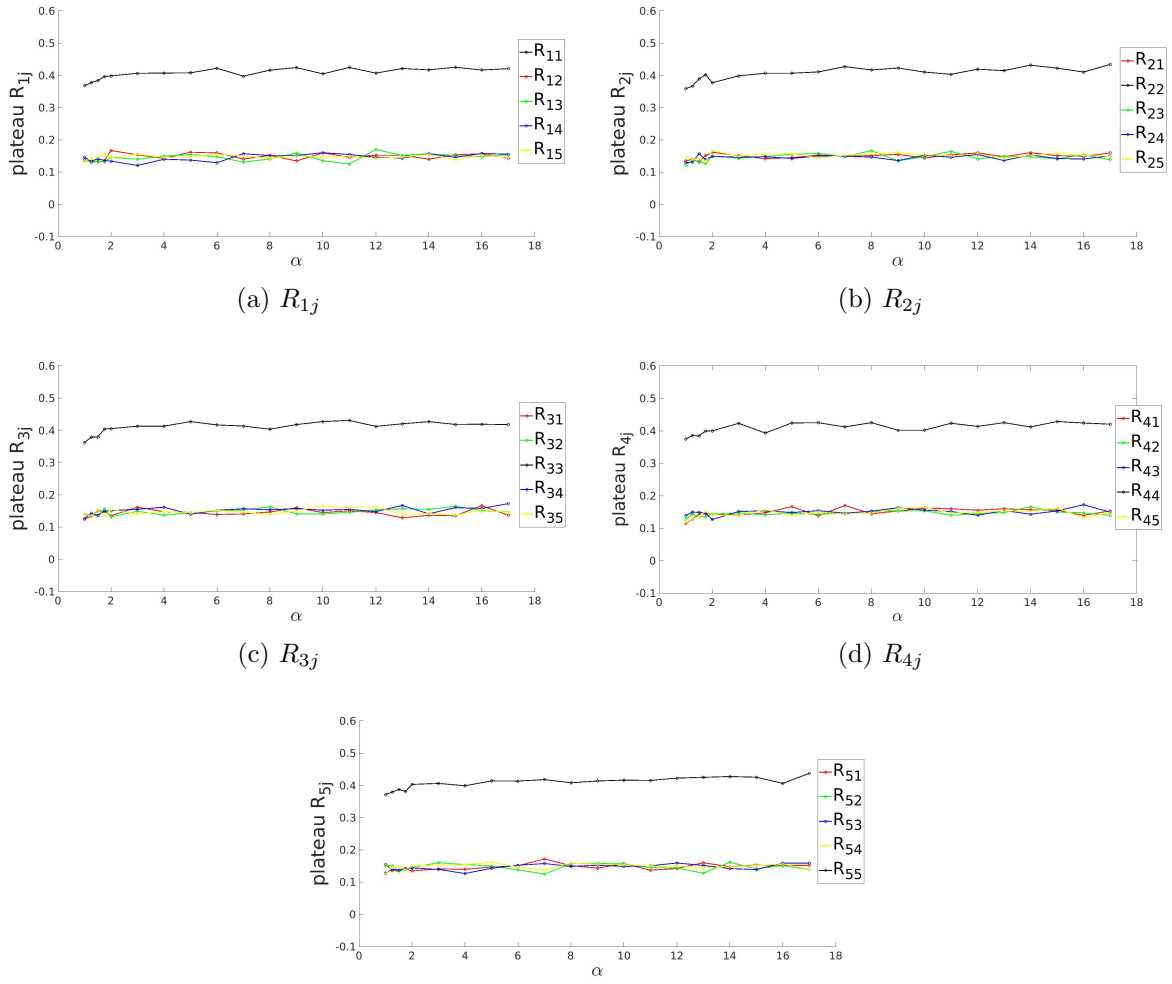

(a) R_{1j} (b) R_{2j}

(c) R_{3j} (d) R_{4j}

(e) R_{5j}

Figure 3.4: Row-wise plot of student-teacher overlap order parameter matrix at the plateau of ϵ_g. The diagonal elements of R_{ij} (in black) saturate at 0.5 and off-diagonal elements saturate at 0.1, signaling poor generalization.

Applying the same conditions as $K = 2$ (3.1.1) for 5 hidden units, during the learning process the neural network gets stuck in a plateau state and the decrease in the loss appears to stagnate. This is the plateau phenomenon and it manifests itself in many learning tasks (Ainsworth and Shin 2020). For example, in figure (3.3a), the learning curve for R_{1j} appears to be stuck in plateau till $\alpha \approx 2$.

For higher alphas, these plateau states are overcome and as per theory from (Oostwal et al. 2021) predicts that a phase transition occurs in this regime. Each student vector largely overlaps with exactly one teacher vector. This represents the specialized phase where $R_{ij} = 1$ for $i = j$ and zero for $i \neq j$ which is evident from (3.3a).

3.3.3 Anti-specialized Converged state for K=5 ReLU system

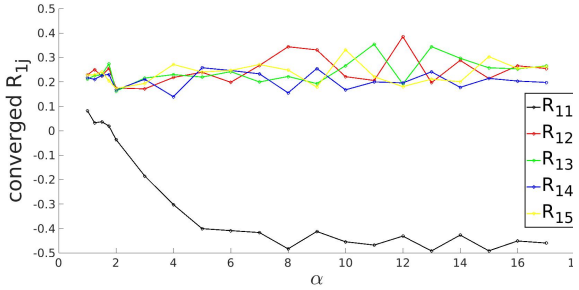

(a) R_{1j}

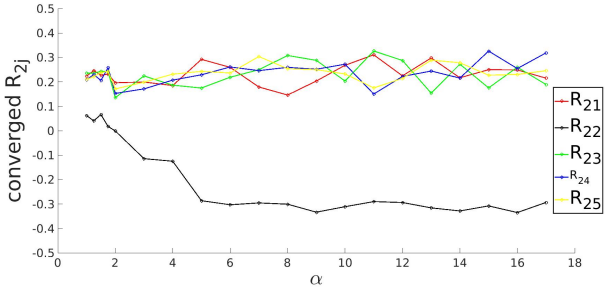

(b) R_{2j}

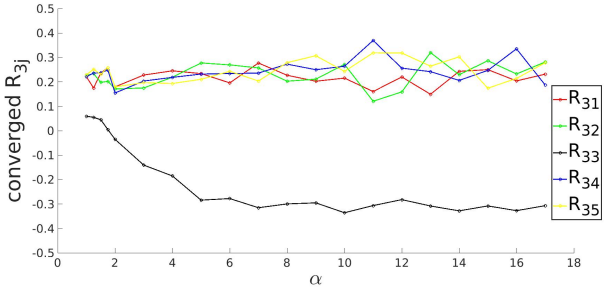

(c) R_{3j}

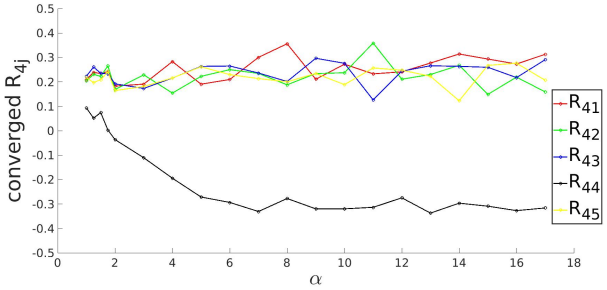

(d) R_{4j}

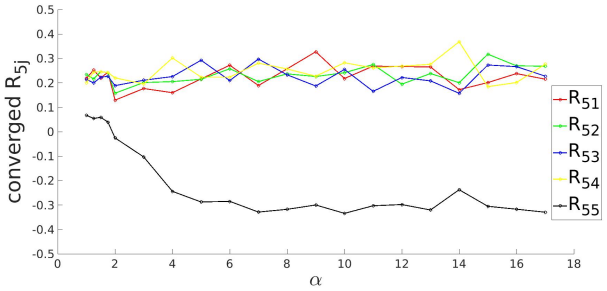

(e) R_{5j}

Figure 3.5: Row-wise plot of student-teacher overlap order parameter matrix at the converged ϵ_g for anti-specialization initialization. The diagonal elements of R_{ij} (in black) approach the value of -0.5 and off-diagonal elements saturate at 0.1, as alpha increases. The ϵ_g corresponding to these order parameters is shown in fig3.7, where a good reduction is seen as a function of alpha. This implies that these anti-specialized states are a good solution of the learning problem.

3.3.4 Antispecialized plateau state for K=5 ReLU system

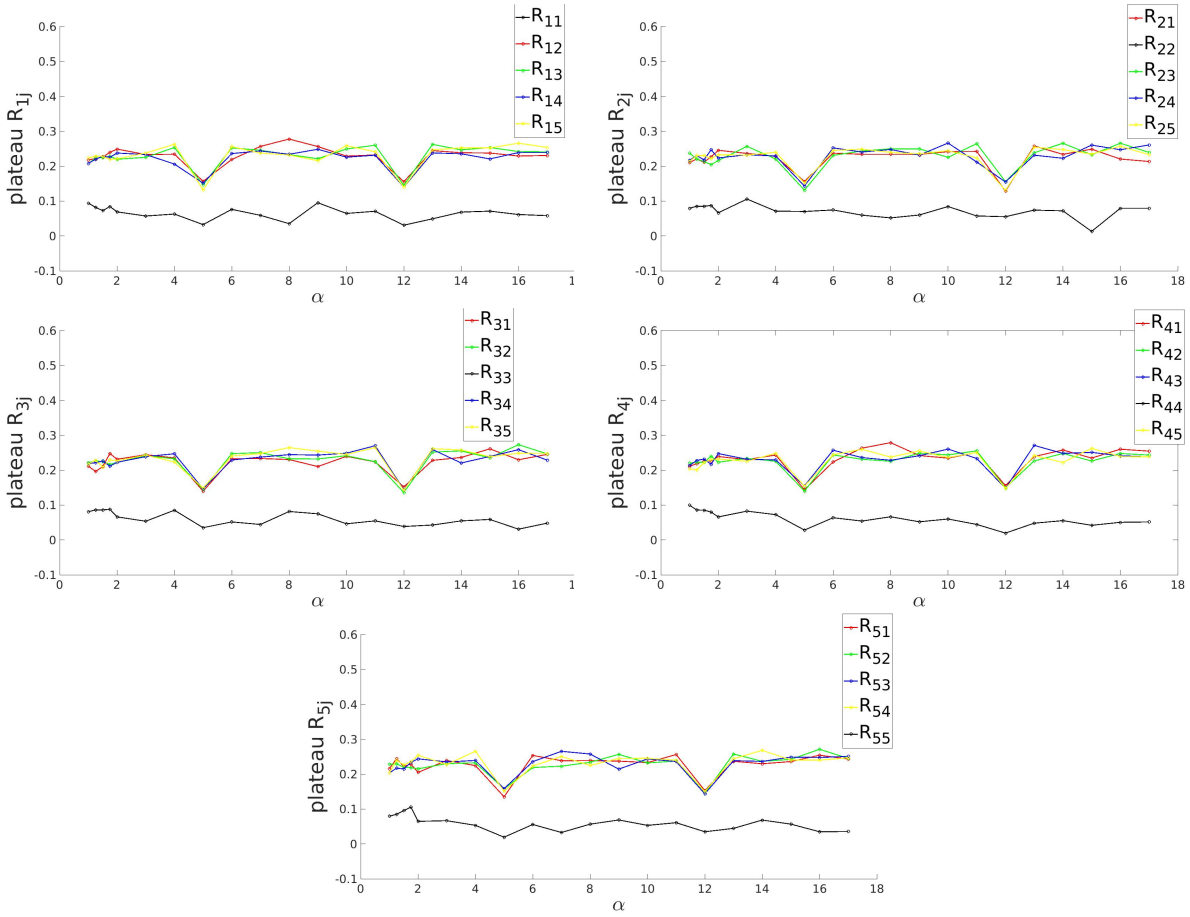

Figure 3.6: Row-wise plot of student-teacher overlap order parameter matrix at the plateau ϵ_g for anti-specialized initialization. The diagonal elements of R_{ij} (in black) remain at 0 as alpha progresses and the off-diagonal elements remain at 0.2, this correlates to almost no reduction in ϵ_g.

Based on the initial conditions (3.1.2) for 5 hidden units using ReLU the learning process of the neural network appears to be initially stuck in a plateau and the decrease in the loss stagnates in this region. For example, in figure (3.5a), the learning curve for R_{1j} appears to be stuck in a plateau till $\alpha \approx 2$. As the α increases beyond this, the plateau states are overcome and as per theory from (Oostwal et al. 2021) it is predicted that the phase transition occurs in this α regime. The unspecialized state is replaced by negatively specialized state (anti-specialized) (3.5). Each student vector largely negatively overlaps with the corresponding teacher vector which represents the converged R_{ij} and weakly positively with the remaining teacher vectors (positive dot product). In figure (3.5a) the converged R_{1j} value for $\alpha = 17$ is -0.4599 while the remaining $R_{1j} \approx 0.3$.

3.3.5 Generalization error for K=5 ReLU

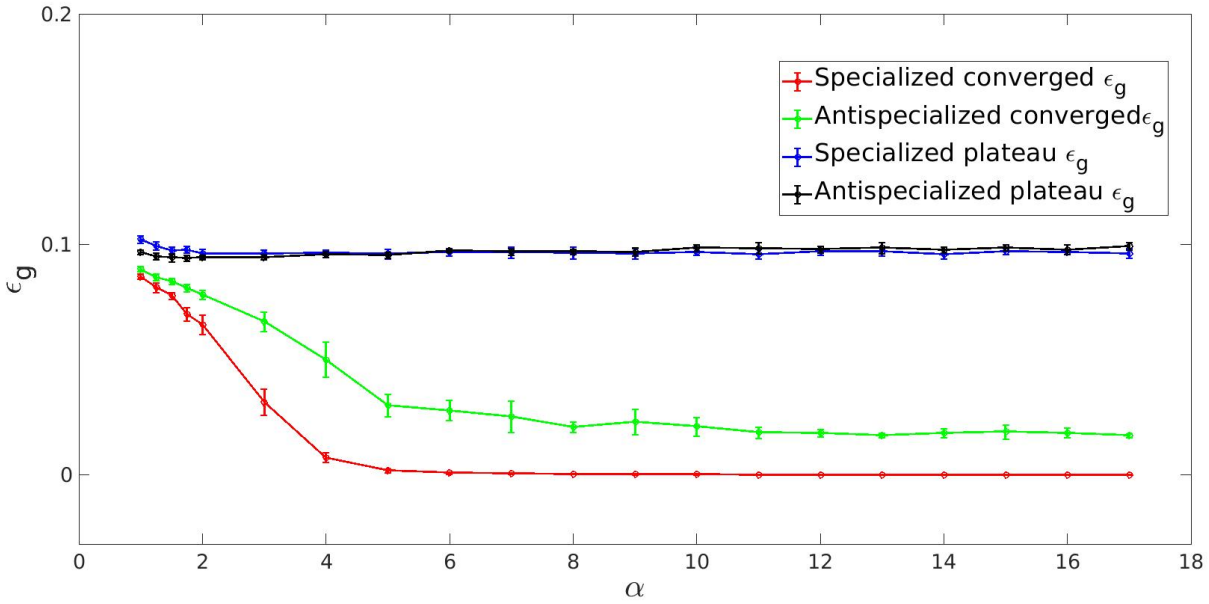

Figure 3.7: ϵ_g as a function of α for converged & plateau states using ReLU activation function for $K = 5$ hidden units. For both states, two different initial conditions lead to specialization and anti-specialization of hidden units respectively. The anti-specialized state performs good but worse than the specialized state.

It is important to note that we have used $N = 600$ in the figure above, therefore the same α w.r.t the specialized state actually realizes a larger dataset size P. The generalization error for the anti-specialized case is poor as compared to the specialized case as seen in figure (3.7). There is a definitive drop in the ϵ_g after $\alpha \approx 2$, however it is not as steep for anti-specialized as it is for the specialized case. For higher $\alpha = 17$ the converged anti-specialized ϵ_g is 0.0171 as compared to converged specialized $\epsilon_g = 1.2189e - 04$. There is a qualitative similarity with the theoretical results from (Oostwal et al. 2021) where the calculations are done for $N \to \infty$. However in this limit, there is no difference between the anti-specialized and specialized ϵ_g. Moreover, diagonal elements of R approach -1. This could be because we have not found the correct initial conditions which leads to anti-specialization or because in simulations N is not large enough.

3.3.6 Converged state for K=5 Sigmoid

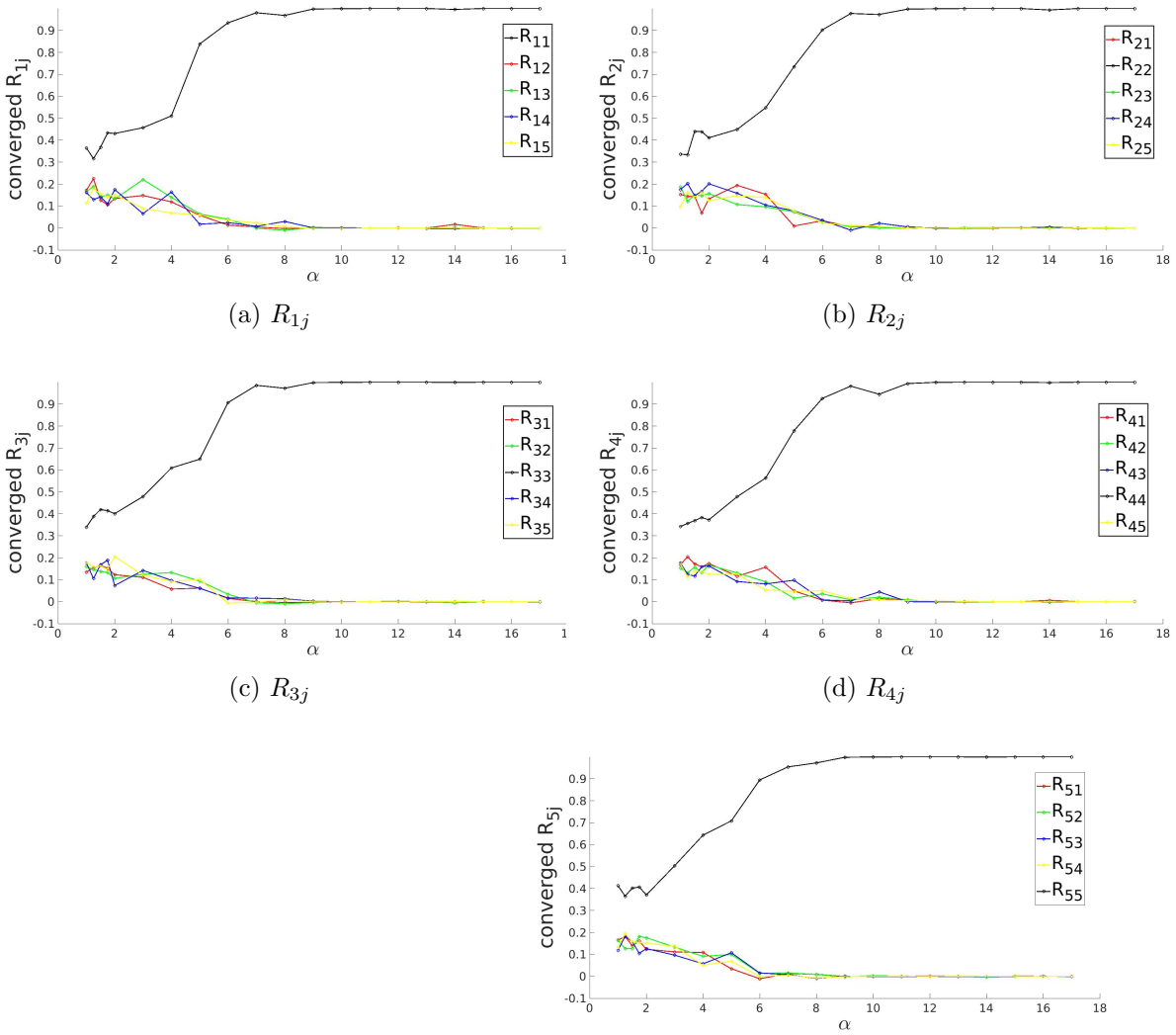

(a) R_{1j} (b) R_{2j}

(c) R_{3j} (d) R_{4j}

(e) R_{5j}

Figure 3.8: Row-wise plot of student-teacher overlap order parameter matrix at the converged ϵ_g. The diagonal elements of R_{ij} (in black) approach the value of 1 and off-diagonal elements approach 0, as alpha increases signalling specialization. Compared to the ReLU activation function in fig3.3, the specialization is achieved at a slightly larger α.

3.3.7 Plateau state for K=5 Sigmoid

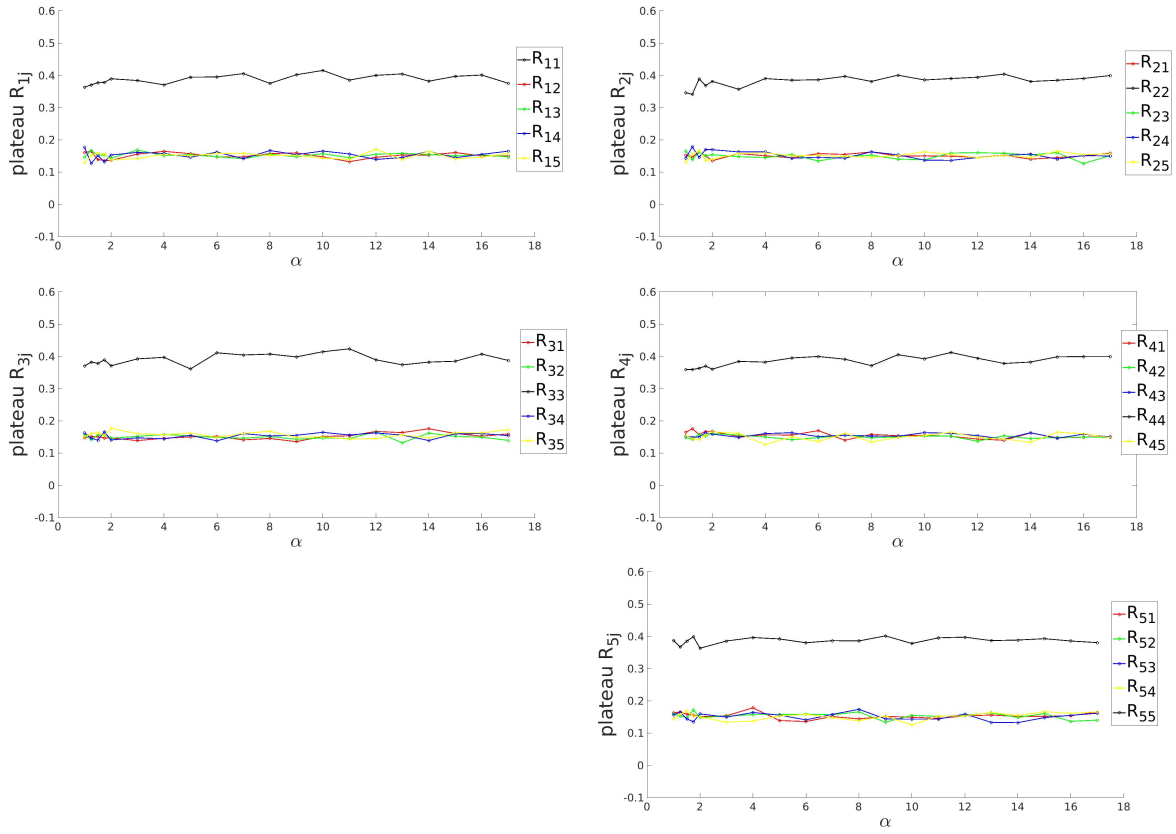

Figure 3.9: Row-wise plot of student-teacher overlap order parameter matrix at the plateau of ϵ_g. The diagonal elements of R_{ij} (in black) saturate at 0.4 and off-diagonal elements saturate at 0.2, signaling poor generalization.

For $\alpha \approx 3$ and smaller the students are still unspecialized as seen in figure (3.8a). After this, the students starts to learn which from the theory (Oostwal et al. 2021) refers to a phase transition. It is interesting to note that this transition appears some what in a jump between $\alpha \approx 4$ to $\alpha \approx 6$. For higher α the student specializes as $R_{ii} \to 1$ for the corresponding student-teacher vectors and $R_{ij} \to 0$ for the remaining.

3.3.8 Generalization error for K=5 Sigmoid

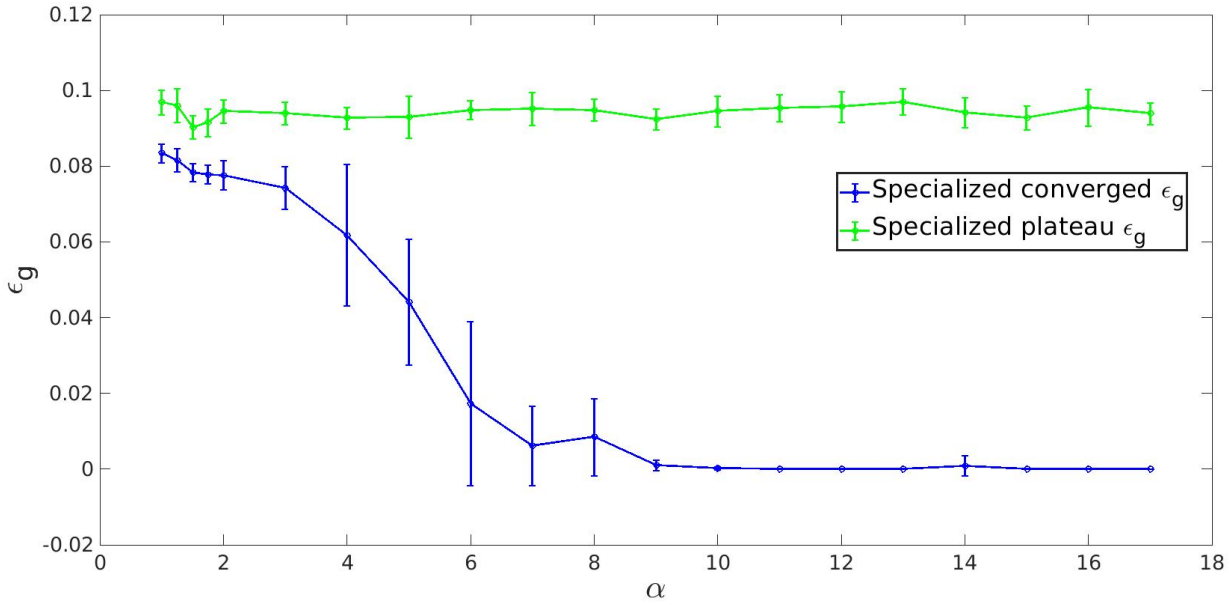

Figure 3.10: ϵ_g as a function of α for converged and plateau states using sigmoid activation function for $K = 5$ hidden units. The initial conditions lead to specialization of the hidden units.

The generalization error decreases slowly till $\alpha \approx 3$ after which, the decrease in the ϵ_g is rapid and it goes to zero for higher αs. In this case, for $\alpha = 3$, ϵ_g is 0.07429 and for $\alpha = 17$, ϵ_g is $6.969e - 06$.

Chapter 4

Summary and Discussion

In this section we summarize the key insights generated from our simulations described in the previous section.

- For $K = 2$ ReLU system, the unspecialized state for the student teacher overlap matrix (2.18) where R and S barely vary lasts till $\alpha \approx 3$. For $\alpha \approx 4$ and greater, R approaches 1 while S approaches 0 and they signal that the system has entered a specialized state. Similar trend can be qualitatively observed in Fig 3 from theory in (Oostwal et al. 2021) where at $\alpha \approx 6.1$ a phase transition occurs. Before this phase transition both R and S take the same values denoting an unspecialized state and after this phase transition R and S bifurcate and approach 1 and 0 respectively, denoting a specialized state. At this α a kink occurs and a rapid drop in the ϵ_g follows. The theory in (Oostwal et al. 2021) is based on statistical mechanics of equilibrium and considers $N \to \infty$. However, we simulate for $N = 100$ and disregard the temperature regime. Moreover, the use of stochastic gradient descent gives rise to the variation in ϵ_g at every alpha, and hence this kink could not be observed in the simulations (see error bars in 3.10 (a)).

- For $K = 2$ sigmoid system, the trends in R, S and ϵ_g remain qualitatively similar in both simulations and theory. In this system the phase transition (Fig 2 Oostwal et al. 2021) occurs at $\alpha \approx 23.7$ as compared to $\alpha \approx 6.1$ for the ReLU system. In our simulations for the $K = 2$ Sigmoidal system, we observe that the onset of specialization happens at a slightly larger α than $K = 2$ ReLU system, however the difference between the αs is much smaller compared to the one reported in theory.

- For $K = 5$ ReLU system, similar trends for R, S and ϵ_g as compared to $K = 2$ ReLU system persists in terms of qualitative agreement with the theory (where K = 10). We observe the existence of an anti-specialized state for $K = 5$ ReLU system that achieves low ϵ_g in line with the theory. In the simulations, the anti-specialized state does not achieve the minimum overlap of $R_{ii} = -1$ but achieves an $R_{ii} = -0.5$, this could be either because a larger K is needed or because a different initial condition is needed, to observe a full anti-specialization. We also observe that the anti-specialized state did not perform as good as the specialized state, Fig 4 from theory predicts that for the limit $K \to \infty$, the performance of both types of states becomes the same. We did not observe such an anti-specialized state that performs well in reducing ϵ_g for $K = 5$ sigmoidal system, this is in line with the theory.

In conclusion key theoretical insights from (Oostwal et al. 2021) such as observation of a phase transition, difference between ReLU and Sigmoidal activation functions and anti-specialization in $K = 5$ ReLU system are reflected in our simulation results.

4.1 Outlook

The next steps in the project could include:

- Finding initial-conditions that make the student reach minimum overlap with teacher ($R_{ii} = -1$) while still reducing ϵ_g to below acceptable level. This needs to be done for ReLU activation function, as it is known from theory that for the sigmoid activation function anti-specialized state does not exist.
- Studying systems with larger number of hidden units (K) is interesting, as here the performance gap between specialized and anti-specialized state is expected to be smaller.

References

Ahr, Martin, Biehl, Michael, and Urbanczik, Robert (Dec. 1998). "Statistical physics and practical training of soft-committee machines". In: *The European Physical Journal B* 10. DOI: 10.1007/s100510050889.

Ainsworth, Mark and Shin, Yeonjong (July 2020). "Plateau Phenomenon in Gradient Descent Training of ReLU networks: Explanation, Quantification and Avoidance". In:

Angelov, P. and Sperduti, A. (2016). "Challenges in Deep Learning". In: *ESANN*.

Berger, James O (1985). *Statistical decision theory and Bayesian analysis; 2nd ed.* Springer Series in Statistics. New York: Springer. DOI: 10.1007/978-1-4757-4286-2. URL: https://cds.cern.ch/record/1327974.

Biehl, Michael, Schlosser, Enno, and Ahr, Martin (Oct. 1998). "Phase Transitions in Soft-Committee Machines". In: *Computer Physics Communications* 121-122. DOI: 10.1209/epl/i1998-00466-6.

Gibbs, J. Willard (Josiah Willard) (1902). *Elementary principles in statistical mechanics developed with especial reference to the rational foundation of thermodynamics*. New York :C. Scribner, p. 236.

Golub, Gene H. and Van Loan, Charles F. (1996). *Matrix Computations*. Third. The Johns Hopkins University Press.

Goodfellow, Ian, Bengio, Yoshua, and Courville, Aaron (2016). *Deep Learning*. http://www.deeplearningbook.org. MIT Press.

Hahnloser, Richard, Sarpeshkar, Rahul, Mahowald, Misha, Douglas, Rodney, and Seung, H. (July 2000). "Digital selection and analogue amplification coexist in a cortex-inspired silicon circuit". In: *Nature* 405, pp. 947–51. DOI: 10.1038/35016072.

Kelly, Henry J. (1960). "Gradient Theory of Optimal Flight Paths". In: *ARS Journal* 30.10, pp. 947–954. DOI: 10.2514/8.5282. eprint: https://doi.org/10.2514/8.5282. URL: https://doi.org/10.2514/8.5282.

Krogh, Anders and Hertz, John A. (1992). "A Simple Weight Decay Can Improve Generalization". In: *Advances in Neural Information Processing Systems 4*. Ed. by John E. Moody, Steve J. Hanson, and Richard P. Lippmann. San Francisco, CA: Morgan Kaufmann, pp. 950–957. URL: ftp://ftp.ci.tuwien.ac.at/pub/texmf/bibtex/nips-4.bib.

LeCun, Yann, Bengio, Y., and Hinton, Geoffrey (May 2015). "Deep Learning". In: *Nature* 521, pp. 436–44. DOI: 10.1038/nature14539.

Michiel Straat Michael Biehl, Kerstin Bunte (Sept. 2018). "On-line learning in neural networks with ReLU activations". In:

Oostwal, Elisa, Straat, Michiel, and Biehl, Michael (2021). "Hidden unit specialization in layered neural networks: ReLU vs. sigmoidal activation". In: *Physica A: Statistical Mechanics and its Applications,* Volume 564. DOI: https://doi.org/10.1016/j.physa.2020.125517.

Prajit Ramachandran Barret Zoph, Quoc V. Le (2017). "Searching for Activation Functions". In:

Robbins, H. and Monro, S. (1951). "A stochastic approximation method". In: *Annals of Mathematical Statistics* 22, pp. 400–407.

Ruder, Sebastian (2016). *An overview of gradient descent optimization algorithms.* URL: http://arxiv.org/abs/1609.04747.

Rumelhart, David E., Hinton, Geoffrey E., and Williams, Ronald J. (1986). "Learning Representations by Back-propagating Errors". In: *Nature* 323.6088, pp. 533–536. DOI: 10.1038/323533a0. URL: http://www.nature.com/articles/323533a0.

Saad, David and Solla, Sara (Nov. 1995). “On-line learning in soft committee machines”. In: *Physical review. E, Statistical physics, plasmas, fluids, and related interdisciplinary topics* 52, pp. 4225–4243. DOI: 10.1103/PhysRevE.52.4225.

Appendix A

Appendix Chapter

A.1 Appendix section

The ReLU activation function is represented in terms of order parameters (Michiel Straat 2018) as described in 2.18 , 2.16 the teacher-teacher overlap is represented as T_{ij}, it is also the model parameter.

$$\begin{aligned}\epsilon_g = \frac{1}{2K}\sum_{i,j=1}^{K}\Big(\frac{Q_{ij}}{4} + \frac{\sqrt{Q_{ii}Q_{jj} - Q_{ij}^2} + Q_{ij}\sin^{-1}\Big[\frac{Q_{ij}}{\sqrt{Q_{ij}Q_{jj}}}\Big]}{2\pi}\Big) - \\ \frac{1}{K}\sum_{i=1}^{K}\sum_{j=1}^{M}\Big(\frac{R_{ij}}{4} + \frac{\sqrt{Q_{ii}T_{jj} - R_{ij}^2} + R_{ij}sin^{-1}\Big[\frac{R_{ij}}{\sqrt{Q_{ii}T_{mm}}}\Big]}{2\pi}\Big) \\ + \frac{1}{2K}\sum_{i,j=1}^{M}\Big(\frac{T_{ij}}{4} + \frac{\sqrt{T_{ii}T_{jj} - T_{ij}^2} + T_{ij}\sin^{-1}\Big[\frac{T_{ij}}{\sqrt{T_{ii}T_{jj}}}\Big]}{2\pi}\Big)\end{aligned} \tag{A.1}$$

The Sigmoid activation function is represented in terms of order parameters (Saad and Solla

1995) as described in 2.18 , 2.16.

$$\begin{aligned}\epsilon_g = \frac{1}{\pi}\{ &\sum_{i,j=1}^{K} \sin^{-1} \frac{Q_{ij}}{\sqrt{1+Q_{ii}}\sqrt{1+Q_{jj}}} \\ &+ \sum_{n,m=1}^{M} \sin^{-1} \frac{T_{mm}}{\sqrt{1+T_{nn}}\sqrt{1+T_{mm}}} \\ &-2\sum_{i=1}^{K}\sum_{j=1}^{M} \sin^{-1} \frac{R_{ij}}{\sqrt{1+Q_{ii}}\sqrt{1+T_{jj}}}\}\end{aligned} \tag{A.2}$$